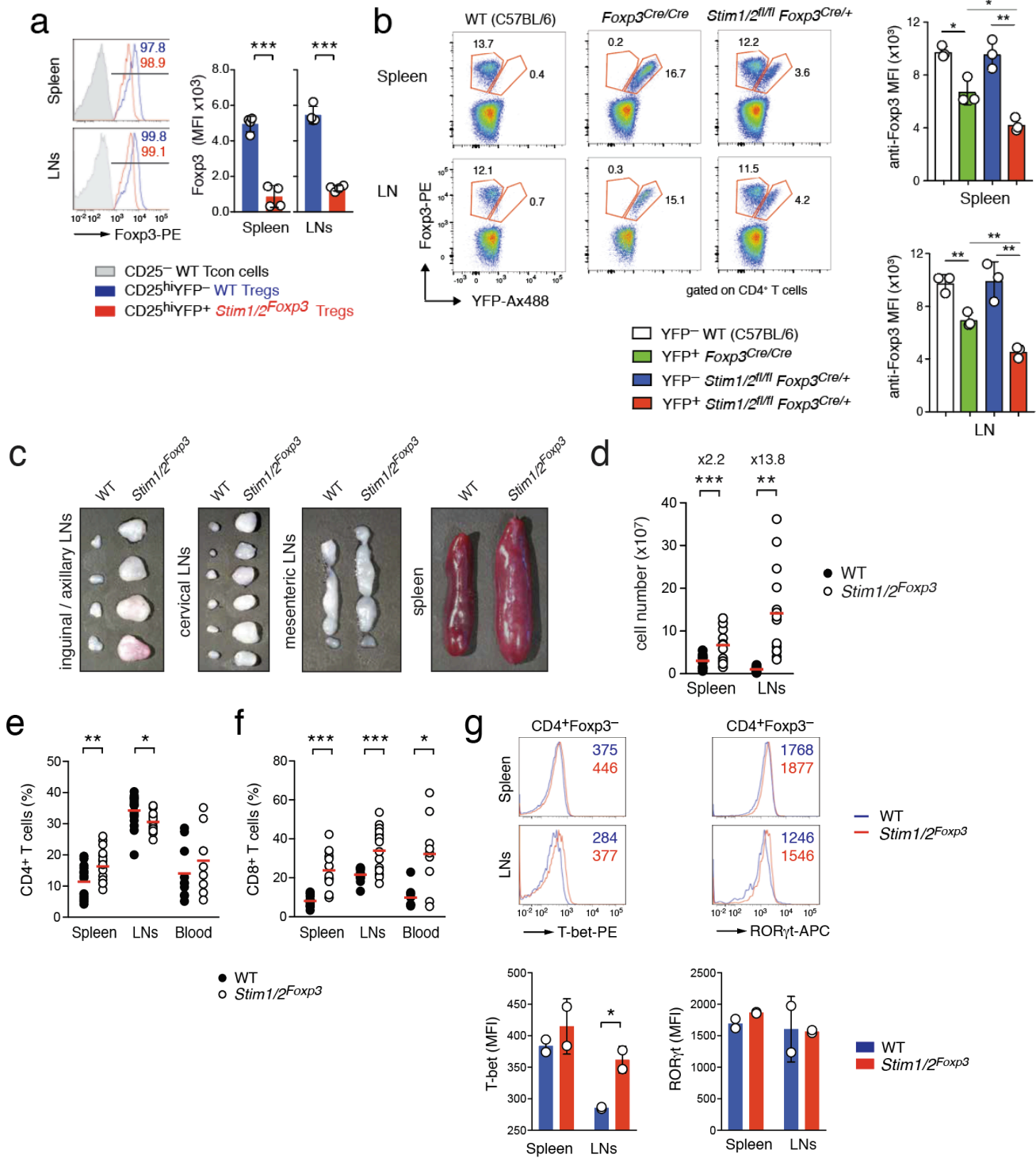


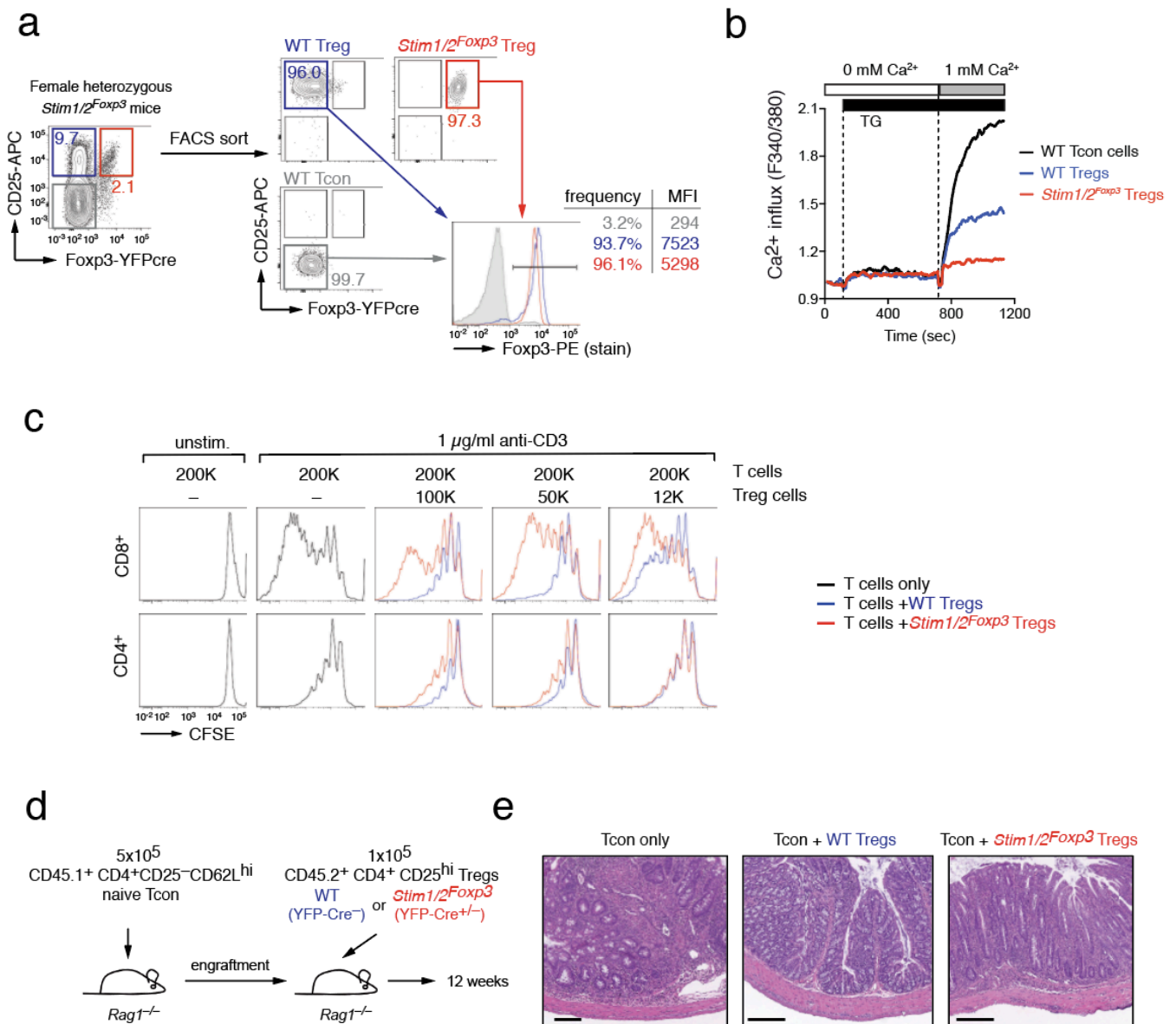
Supplementary Information

Tissue resident and follicular Treg cell differentiation is regulated by CRAC channels

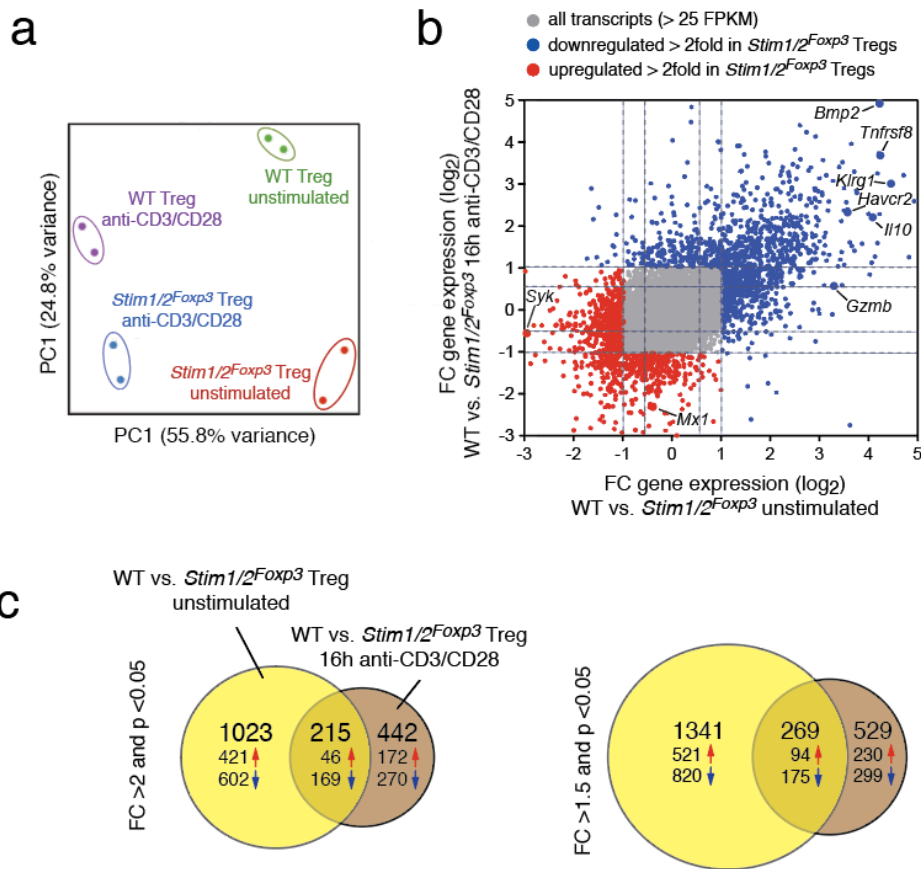
Vaeth et al.



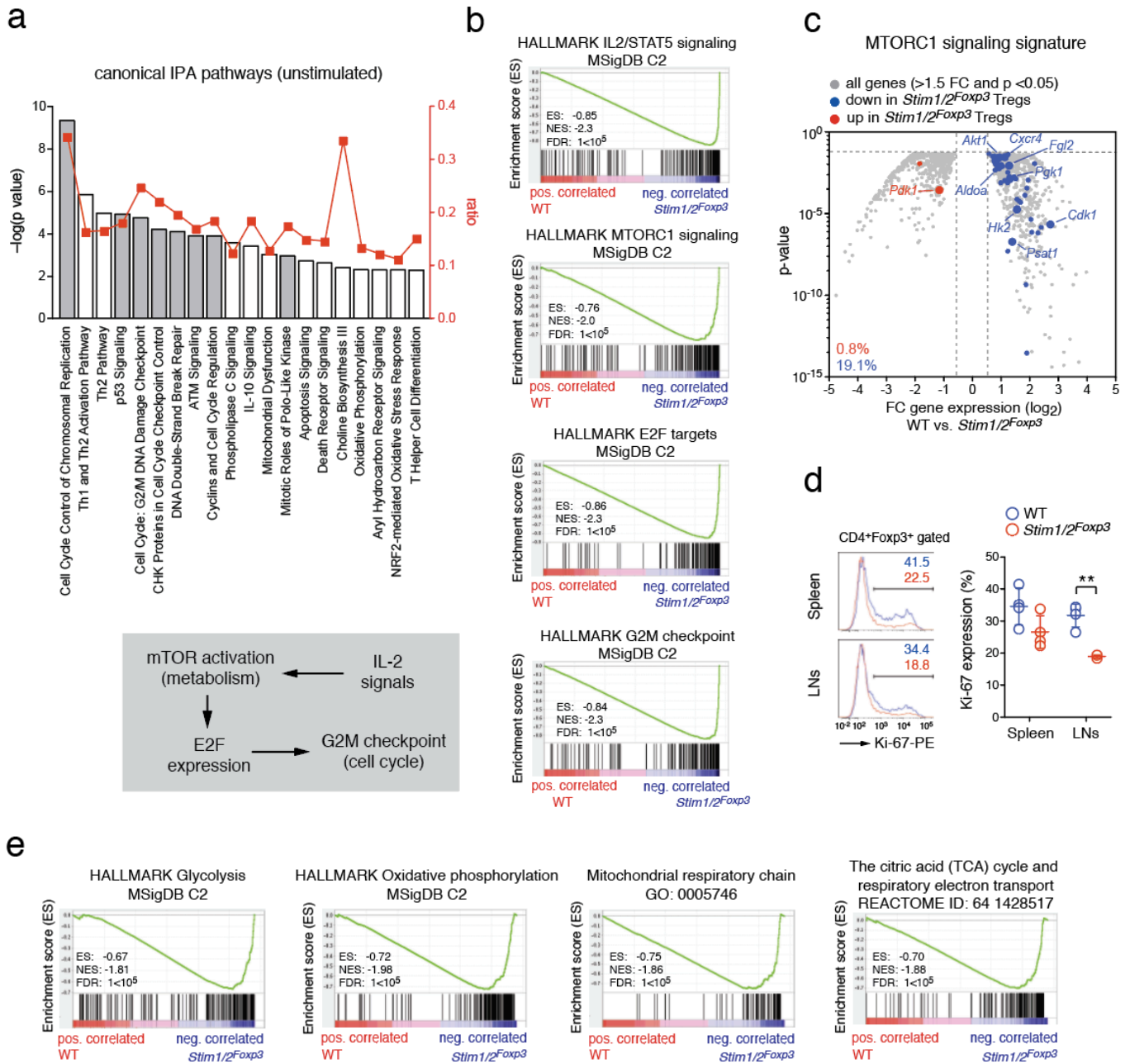
Supplementary Figure 1. Treg-specific deletion of STIM1 and STIM2 causes splenomegaly and lymphadenopathy. (a) Analysis of Fopx3 protein expression in Treg cells of male WT and *Stim1/2*^{Fopx3} mice; mean \pm SEM of 4 mice. (b) Analysis of Fopx3 protein expression in CD4⁺ Treg cells from the spleen and LNs of female C57BL/6 wildtype (WT), *Fopx3*^{YFP^{Cre}/YFP^{Cre} and *Stim1/2*^{fl/fl} *Fopx3*^{YFP^{Cre}/+} mice. Representative flow cytometry plots and means \pm SD from 3 mice per group. (c) Representative pictures of spleen as well as inguinal, axillary, cervical and mesenteric LNs of male WT and *Stim1/2*^{Fopx3} mice. (d) Cellularity of spleen and all LNs of male WT and *Stim1/2*^{Fopx3} mice; mean of 13-14 mice. (e,f) Frequency of CD4⁺ (e) and CD8⁺ (f) T cells in spleen, LNs and blood of male WT and *Stim1/2*^{Fopx3} mice; mean of 9-16 mice. Each dot in b, c and d represents one mouse. (g) Analysis of T-bet and ROR γ t protein levels in CD4⁺ T cells. Representative flow cytometry plots and means \pm SEM of 2-3 mice. Statistical analysis in a,b,d-g by unpaired Student's t-test. *, p<0.05; **, p<0.01, ***, p<0.001.}



Supplementary Figure 2. STIM1 and STIM2 control the immune-suppressive function of Treg cells. **(a)** Gating strategy to isolate WT and *Stim1/2*-deficient *Foxp3*⁺ Treg cells from female heterozygous *Stim1/2*^{Flox3} mice. **(b)** Analysis of SOCE in CD4⁺CD25⁻YFP⁻ conventional T cells (Tcon), CD4⁺CD25⁺YFP⁻ WT Tregs and CD4⁺CD25⁺YFP⁺ Treg cells isolated by flow cytometric cell sorting from the spleen and LNs of female *Stim1/2*^{fl/fl} *Foxp3*^{YFP-Cre/+} mice. 1x10⁵ cells were loaded with Fura-2 and stimulated with thapsigargin (TG) in Ca²⁺ free Ringer solution followed by addition of 1 mM Ca²⁺. Data are representative of 3 mice. **(c)** Suppression of CD4⁺ and CD8⁺ T cell proliferation by WT and *Stim1/2*-deficient Treg cells *in vitro*. 2x10⁵ CFSE-labeled T cells were co-cultured with 1.2x10⁴, 5x10⁴ or 1x10⁵ WT or *Stim1/2*-deficient Treg cells isolated from female heterozygous *Stim1/2*^{Flox3} mice and stimulated with anti-CD3. Proliferation of CD4⁺ and CD8⁺ T cells was analyzed 3 days later by flow cytometry. Data representative of 2 experiments. **(d)** Suppression of CD4⁺ T cells by WT and *Stim1/2*-deficient Treg cells *in vivo*. Adoptive transfer of 5x10⁵ naive CD45.1⁺CD4⁺ Tcon cells to induce inflammatory bowel disease (IBD) in lymphocyte-deficient *Rag1*^{-/-} host mice followed by transfer of 1x10⁵ WT or *Stim1/2*-deficient Treg cells into the same host mice 2-4 weeks later. **(e)** Representative H&E stained colon sections of *Rag1*^{-/-} host mice 12 weeks after transfer of Tcon cells only or Tcon cells together with WT or *Stim1/2*-deficient Treg cells. Images are representative of 3 mice analyzed per cohort.

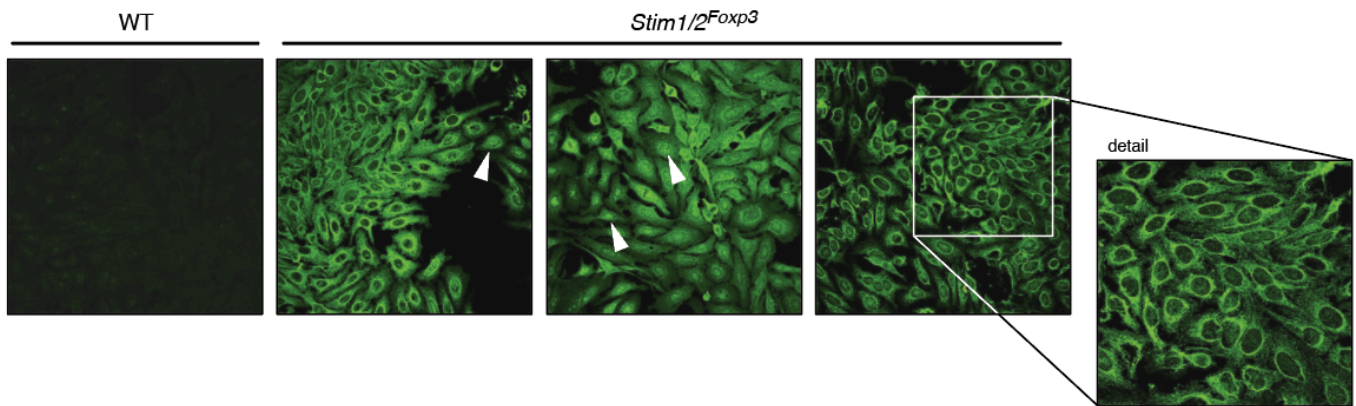


Supplementary Figure 3. Transcriptome analysis of WT and *Stim1/2*-deficient Treg cells. Transcriptional profiling of WT and *Stim1/2*-deficient Treg cells using RNA-sequencing. Spleen and LNs of 12-16 female hemizygous *Stim1/2^{Foxp3}* mice were pooled to isolate YFP⁻ and YFP⁺ Treg cells. WT and *Stim1/2*-deficient Treg cells used for RNA-sequencing were > 93% positive for Foxp3 after sorting (compare with gating strategy shown in Supplementary Figure 2a). **(a)** Principle component analysis (PCA) of unstimulated and anti-CD3/CD28 stimulated WT and *Stim1/2*-deficient Treg cells based on RNA-sequencing data. **(b)** Fold change of differentially expressed genes (DEG) of unstimulated and anti-CD3/CD28 stimulated WT and *Stim1/2*-deficient Treg cells; down- and upregulated genes are depicted in blue and red, respectively. **(c)** Venn diagrams of DEG that are expressed > 2 fold (left panel) and > 1.5 fold (right panel) in unstimulated and anti-CD3/CD28 stimulated WT versus *Stim1/2*-deficient Treg cells. Numbers of genes down- and upregulated are indicated by blue and red arrows, respectively.



Supplementary Figure 4. SOCE controls IL-2 and mTOR signaling in Treg cells. (a) Canonical pathway analysis (IPA) of differentially expressed genes (DEG) in unstimulated WT versus *Stim1/2*-deficient Treg cells. (b) Top four enriched molecular signatures by gene set enrichment analysis (GSEA) of DEG in WT versus *Stim1/2*-deficient Treg cells. (c) Volcano plot of DEG (grey) in unstimulated WT and *Stim1/2*-deficient Treg cells overlaid with up- (red) or downregulated (blue) genes of the 'MTORC1 signaling signature' (Liberzon et al., 2015). (d) Analysis of cell cycle (Ki-67) in Foxp3⁺ Treg cells isolated from the spleen and LNs of male WT and *Stim1/2^{Foxp3}* mice by flow cytometry; mean \pm SEM of 4 mice. (e) Identification of metabolic signatures by GSEA using DEG in unstimulated WT (YFP⁻) versus *Stim1/2*-deficient (YFP⁺) Treg cells from female hemizygous *Stim1/2^{Foxp3}* mice. Statistical analysis in d by unpaired Student's t-test. **, $p < 0.01$.

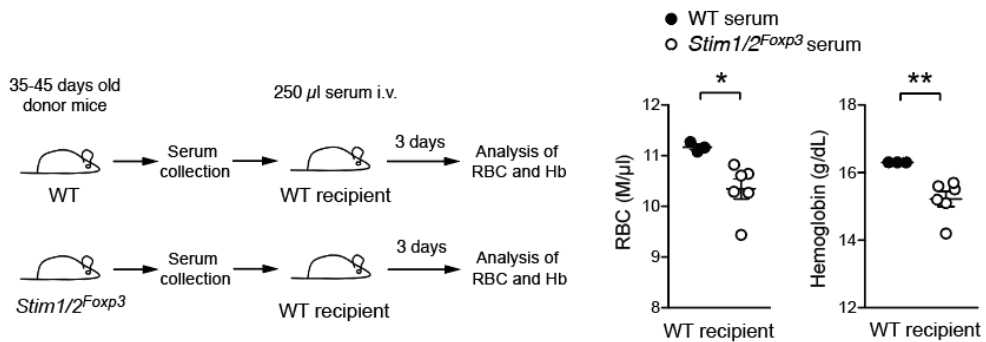
a



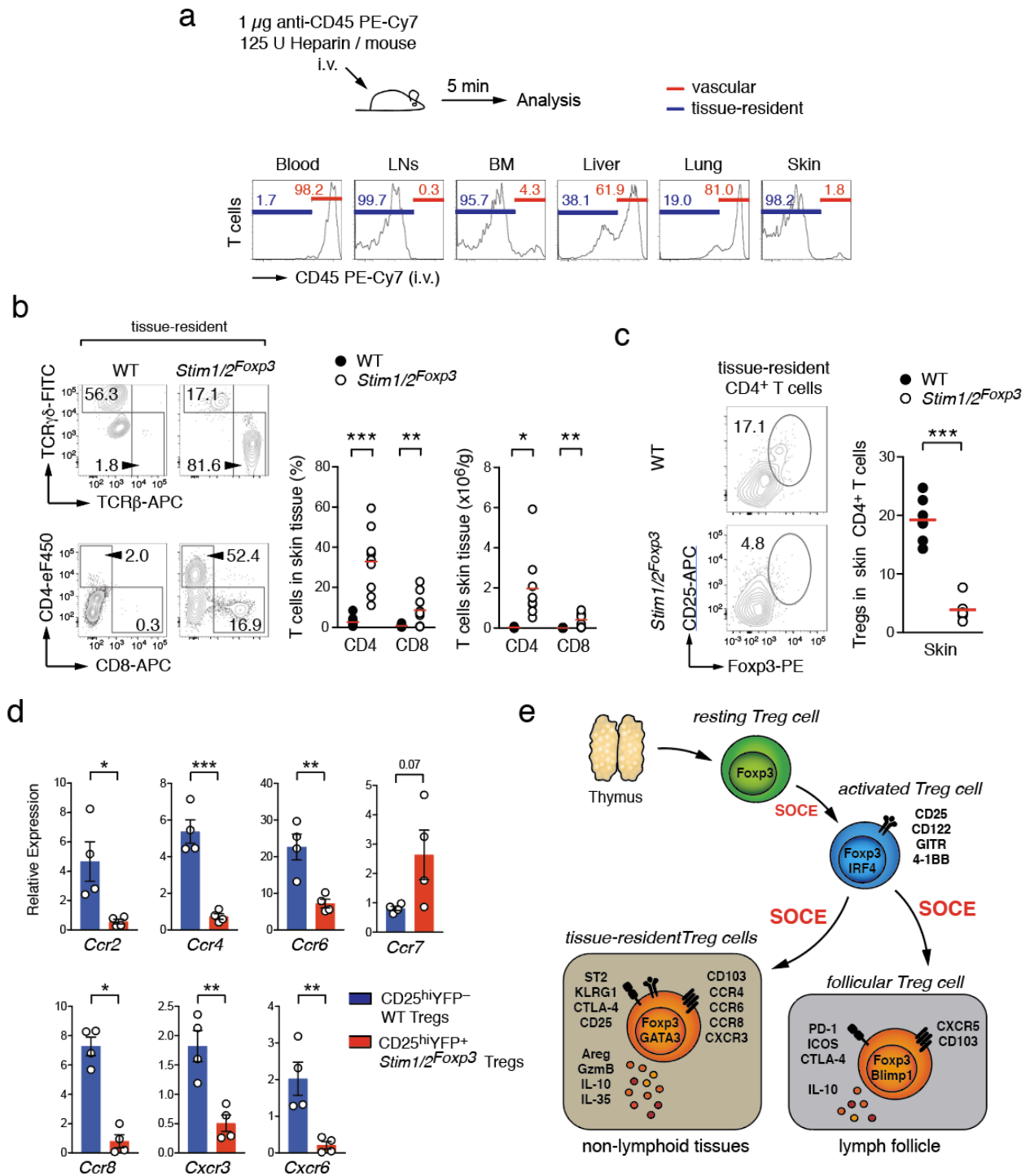
b



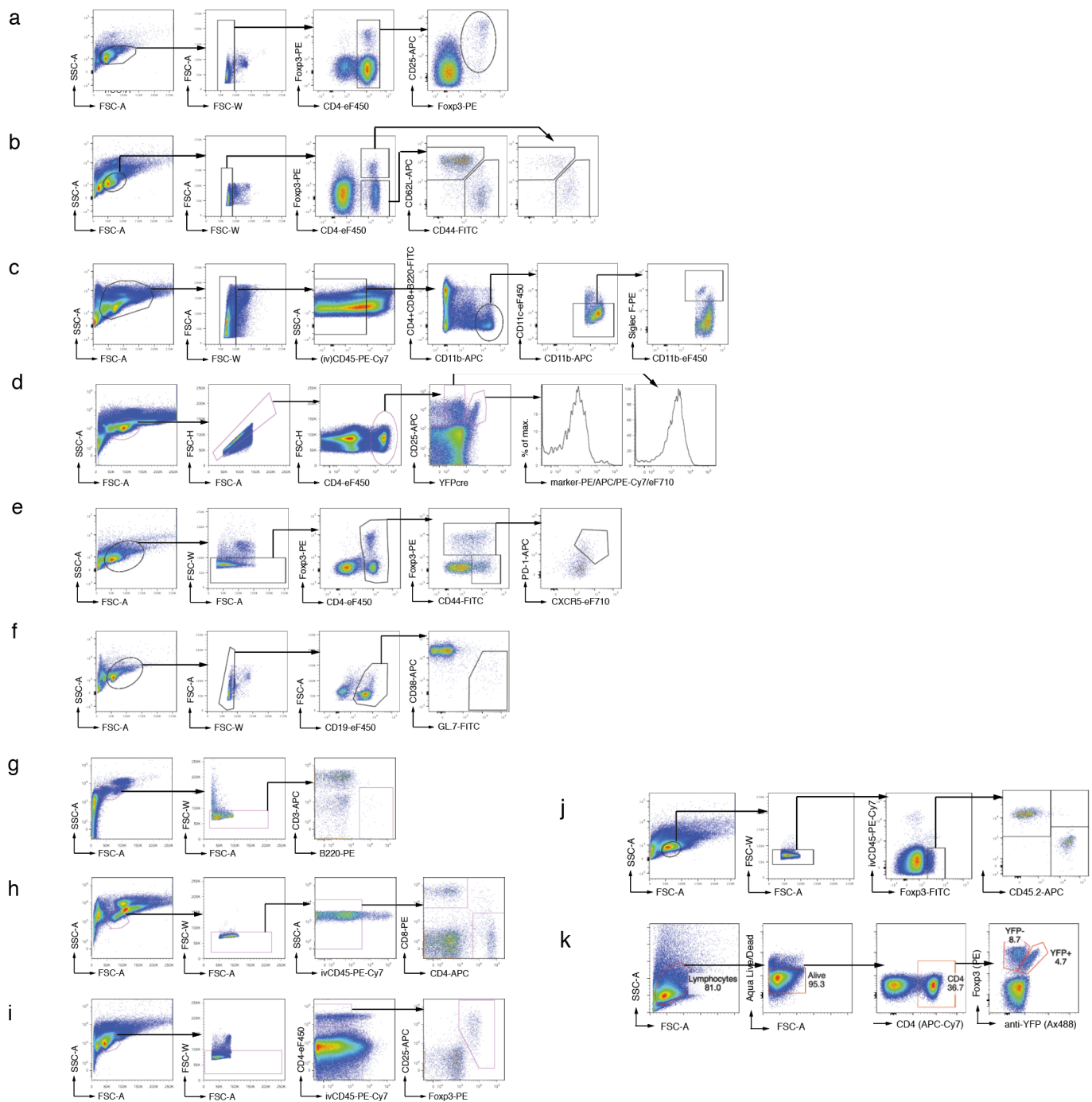
c



Supplementary Figure 5. Treg-specific deletion of STIM1 and STIM2 is associated with autoantibody production. (a) Detection of autoantibodies in the sera of male WT and *Stim1/2^{Foxp3}* mice on HEp-2 cells; representative immunofluorescence images of 6 mice. Sera were diluted 1:50. White arrows indicate cells with positive nuclear staining. The nuclear staining pattern indicates the presence of antinuclear antibodies (ANA), whereas the fine fibrous cytosolic staining pattern is consistent with antimitochondrial antibodies (AMA). (b) Heparinized blood samples of male WT and *Stim1/2^{Foxp3}* mice diluted 1:20 to reveal anemia. (c) Transfer of serum from male WT and *Stim1/2^{Foxp3}* mice into WT recipient mice. RBC counts and hemoglobin levels in the blood of recipient mice 3 days after serum transfusion; means of 3-6 recipient mice. Each dot represents one mouse. Statistical analysis in c by unpaired Student's t-test. *, $p < 0.05$; **, $p < 0.01$.



Supplementary Figure 6. STIM1 and STIM2 regulate tissue-residency of Treg cells and expression of chemokine receptors. (a) Strategy to identify tissue-resident T cells. Intravenous injection of PE-Cy7 labeled anti-CD45 antibody marks intravascular immune cells whereas parenchymal or tissue-resident cells are not stained. (b) Analysis of tissue-resident $\alpha\beta$ and $\gamma\delta$ T cells (upper panel) and CD4⁺ and CD8⁺ T cells (lower panel) in the skin of male WT and *Stim1/2^{Foxp3}* mice by flow cytometry; means of 7-9 mice. (c) Analysis of tissue-resident Foxp3⁺ Treg cells in the skin of male WT and *Stim1/2^{Foxp3}* mice by flow cytometry; means of 6-7 mice. (d) Analysis of *Ccr2*, *Ccr4*, *Ccr6*, *Ccr7*, *Ccr8*, *Cxcr3* and *Cxcr6* gene expression in WT and *Stim1/2*-deficient Treg cells isolated from female heterozygous *Stim1/2^{Foxp3}* mice by qRT-PCR; means \pm SEM of 4 mice. Each dot in b and c represents one mouse. Statistical analysis in b-d by unpaired Student's t-test. *, $p < 0.05$; **, $p < 0.01$, ***, $p < 0.001$. (e) Graphical summary how SOCE controls Treg differentiation into Tfr and tissue resident Treg cells. For details see text.



Supplementary Figure 7. Gating strategies for the flow cytometric detection of immune cells. (a) Detection of Treg cells in Figure 1c. **(b)** Detection of naïve, effector and memory T cells and Treg cells in Figures 1d and 2b. **(c)** Detection of tissue resident eosinophils in Figure 2f. **(d)** Analysis of expression of transcription factors and cell surface markers on Treg cells in Figures 2c, 3g, 6b and Supplementary Figures 1b,g, 2a and 4d. **(e)** Analysis of CXCR5^{hi} Tfr cells in Figure 4b. **(f)** Determination of the frequency of GC B cells in Figure 4d. **(g)** Strategy to verify B cell depletion after anti-CD20 treatment in Figure 4j. **(h,i)** Identification of tissue resident CD4⁺ and CD8⁺ T cells (h) and Treg cells (i) after *in vivo* labelling of intravascular lymphocytes with anti-CD45-PE-Cy7 in Figures 5c,d, 6a,b and Supplementary Figures 6b,c. **(j)** Analysis of chimerism of tissue resident Treg cells in Figure 6d. **(k)** Determination of the frequency of YFP⁺ and YFP⁻ Treg cells in female heterozygous *Stim1/2*^{Foxp3} mice in Supplementary Figure 1b.

Supplementary Table 1. Autoimmunity and AIHA in SOCE-deficient patients.

Mutation	Autoimmunity	Tregs in blood	Outcome	Reference
<i>ORAI1 p.R91W</i>	n.r.	n.t.	dead (11 mo)	1, 11, 12, 13
<i>ORAI1 p.R91W</i>	ANA, dsDNA autoAbs	reduced	alive after HSCT	1, 11, 12, 13
<i>ORAI1 p.A88SfsX25</i>	Neutropenia, thrombocytopenia	n.t.	dead (11 mo)	1
<i>ORAI1 p.A103E/L194P</i>	n.r.	n.t.	dead after HSCT	1
<i>ORAI1 p.H165PfsX1</i>	n.r.	n.t.	alive after HSCT	4
<i>ORAI1 p.R270X</i>	n.r.	n.t.	dead (7 mo)	5
<i>ORAI1 p.V181SfsX8</i>	n.r.	n.t.	alive after HSCT	3
<i>ORAI1 p.L194P</i>	AIHA, thrombocytopenia	n.t.	dead (8 mo)	3
<i>ORAI1 p.G98R</i>	AIHA, ANA, cardiolipin autoAbs	reduced	alive after HSCT	3
<i>ORAI1 p.G98R</i>	AIHA, thrombocytopenia, antiphospholipid syndrome	n.t.	dead (2.5 yr)	3
<i>STIM1 p.E128RfsX9</i>	AIHA, thrombocytopenia	reduced	dead after HSCT	6
<i>STIM1 p.E128RfsX9</i>	thrombocytopenia	n.t.	alive after HSCT	6
<i>STIM1 c.1538-1 G>A</i>	AIHA	n.t.	dead (2 yr)	7
<i>STIM1 p.R429C</i>	AIHA, thrombocytopenia, ANA	reduced	alive after HSCT	8
<i>STIM1 p.R429C</i>	AIHA, thrombocytopenia	n.t.	dead (21 mo)	8
<i>STIM1 p.P165Q</i>	Lymphadenopathy, splenomegaly	normal	alive (8 yr)	9
<i>STIM1 p.P165Q</i>	n.r.	normal	alive (21 yr)	9
<i>STIM1 p.L74P</i>	thrombocytopenia	normal	alive (11 yr)	10
<i>STIM1 p.L74P</i>	n.r.	n.t.	alive (21 yr)	10

Supplementary Table 2. Antibodies used for flow cytometry.

Mouse antigen	Clone	Conjugates	Source	Dilution
B220	RA3-6B2	PE, eFluor450	eBioscience	1:400
CD3e	2C11	APC, eFluor450	eBioscience	1:400
CD4	GK1.5	FITC, AlexaFluor488, PE, APC, eFluor450	eBioscience	1:400
CD8	53-6.7	FITC, AlexaFluor488, PE, APC, eFluor450	eBioscience	1:400
CD11b	M1/70	eFluor450	eBioscience	1:200
CD11c	N418	APC	Biolegend	1:200
CD25	PC61.5	APC	eBioscience	1:400
CD38	90	APC	eBioscience	1:200
CD39	24DMS1	PE-Cy7	eBioscience	1:200
CD44	IM7	FITC, PE, eFluor450	eBioscience	1:400
CD45	30-F11	PE-Cy7	eBioscience	1:400
CD45.1	A20	FITC, APC, eFluor450	eBioscience	1:400
CD45.2	104	PE, APC, eFluor450	eBioscience	1:400
CD62L	MEL-14	APC	eBioscience	1:400
CD103	2 E7	APC	eBioscience	1:200
CXCR5	SPRCL5	eFluor710	eBioscience	1:100
FoIR4	eBio12A5	APC	eBioscience	1:200
Foxp3	FJK-16s	PE, APC	eBioscience	1:100
GATA3	TWAJ	APC	eBioscience	1:100
TCR b	H57-597	APC	eBioscience	1:200
TCR gd	UC7-13D5	FITC	eBioscience	1:200
GL7	GL7	FITC, AlexaFluor488	eBioscience	1:100
ICOS	C398.4A	APC	eBioscience	1:400
IFNg	XMG1.2	PE, APC	eBioscience	1:100
IgG	polyclonal (Fab) ₂ fragment	FITC	eBioscience	1:100
IL-17A	eBio17B7	APC	eBioscience	1:100
Ki-67	16A8	PE, eFluor450	eBioscience	1:200
KLRG1	2F1	eFluor710	eBioscience	1:200
Ox-40	OX86	APC	eBioscience	1:200
PD-1	RMP1-30	APC	eBioscience	1:400
Siglec F	E50-2440	PE	BD Pharmingen	1:200
ST2 (IL-33R)	RMST2-2	APC	eBioscience	1:50
Ter119	TER-119	PE	eBioscience	1:200
GFP	FM264G	AlexaFluor488	Biolegend	1:100

Supplementary Table 3. Primers for realtime PCR.

Mouse gene	Forward primer	Reverse primer
<i>Foxp3</i>	CACCCAGGAAAGACAGCAACC	GCAAGAGCTCTTGCCATTGA
<i>Stim1</i>	ATTCGGCAAACCTCTGCTTC	GGCCAGAGTCTCAGCCATAG
<i>Stim2</i>	TCGAAGTGGACGAGAGTGATG	TTTCCACTGTTCCACAAATCC
<i>Ccr2</i>	AGCACATGTGGTGAATCCAA	TGCCATCATAAAGGAGCCA
<i>Ccr4</i>	GGGTACCAGCAGGAGAAGC	CGACGGCATTGCTTCATAG
<i>Ccr6</i>	TTGAATGGCAGACACTCACAG	GGAGCCTGGATAACCACTGA
<i>Ccr7</i>	GTCTCTCTCCAGCTAGCCCA	CAAACAGGAGCTGATGTCCA
<i>Ccr8</i>	GCGGTGAAGAAATCAGGGTA	CTCAGAAGAAAGGCTCGCTC
<i>Cxcr3</i>	TCTCGTTTTCCCATAAATCG	AGCCAAGCCATGTACCTTGA
<i>Cxcr6</i>	AAATCTCCCTCGTAGTCCCC	TGGAACAAAGCTACTGGGCT
<i>18S</i>	CGGCGACGACCCATTGGAAC	GAATCGAACCCCTGATTCCCCGT
<i>Gapdh</i>	TTGATGGCAACAATCTCCAC	CGTCCCCTAGACAAAATGGT

Supplementary References

1. McCarl, C.A. *et al.* ORAI1 deficiency and lack of store-operated Ca²⁺ entry cause immunodeficiency, myopathy, and ectodermal dysplasia. *J Allergy Clin Immunol* **124**, 1311-1318 e1317 (2009).
2. Vaeth, M. *et al.* Store-Operated Ca Entry in Follicular T Cells Controls Humoral Immune Responses and Autoimmunity. *Immunity* (2016).
3. Lian, J. *et al.* ORAI1 mutations abolishing store-operated Ca(2+) entry cause anhidrotic ectodermal dysplasia with immunodeficiency. *J Allergy Clin Immunol* (2017).
4. Chou, J. *et al.* A novel mutation in ORAI1 presenting with combined immunodeficiency and residual T-cell function. *J Allergy Clin Immunol* **136**, 479-482 e471 (2015).
5. Badran, Y.R. *et al.* Combined immunodeficiency due to a homozygous mutation in ORAI1 that deletes the C-terminus that interacts with STIM 1. *Clin Immunol* **166-167**, 100-102 (2016).
6. Picard, C. *et al.* STIM1 mutation associated with a syndrome of immunodeficiency and autoimmunity. *N Engl J Med* **360**, 1971-1980 (2009).
7. Byun, M. *et al.* Whole-exome sequencing-based discovery of STIM1 deficiency in a child with fatal classic Kaposi sarcoma. *J Exp Med* **207**, 2307-2312 (2010).
8. Fuchs, S. *et al.* Antiviral and regulatory T cell immunity in a patient with stromal interaction molecule 1 deficiency. *J Immunol* **188**, 1523-1533 (2012).
9. Schaballie, H. *et al.* A novel hypomorphic mutation in STIM1 results in a late-onset immunodeficiency. *J Allergy Clin Immunol* **136**, 816-819 e814 (2015).
10. Parry, D.A. *et al.* A homozygous STIM1 mutation impairs store-operated calcium entry and natural killer cell effector function without clinical immunodeficiency. *J Allergy Clin Immunol* **137**, 955-957 e958 (2016).
11. Feske, S. *et al.* A mutation in Orai1 causes immune deficiency by abrogating CRAC channel function. *Nature* **441**, 179-85 (2006).
12. Feske, S. *et al.* The duration of nuclear residence of NFAT determines the pattern of cytokine expression in human SCID T cells. *J Immunol.* **165**, 297-305 (2000).
13. Feske, S. *et al.* Severe combined immunodeficiency due to defective binding of the nuclear factor of activated T cells in T lymphocytes of two male siblings. *Eur J Immunol.* **26**, 2119-26 (1996).